MSc Environmental Sciences
Research Practice Report

TOX79224

Development of physiologically based kinetic (PBK) model of bobwhite quail

Thitirat Kanokjiraporn[a,1,*], Nico van den Brink[b,1], Nynke Kramer[c,1]

[a]*MSc student in Environmental Sciences*
[b]*Daily supervisor*
[c]*Research practice examiner*
[1]*Toxicology Chair Group, Wageningen University, PO Box PO Box 8000, 6700 EA Wageningen, The Netherlands*

Abstract

Physiologically-based kinetic (PBK) models are powerful tools in toxicology and chemical risk assessment as they simulate the absorption, distribution, metabolism, and excretion (ADME) of chemicals in organisms. This study aimed to develop a PBK model, based on existed chicken (*Gallus gallus domesticus*) PBK model, to simulate the pharmacokinetic profile of fipronil and its metabolite, fipronil sulfone, in bobwhite quail (*Colinus virginianus*), following oral exposure. Physiological and physicochemical parameters for quail were sourced from literature, with some parameters extrapolated from related species where data were unavailable. The model's accuracy was evaluated by comparing predicted concentrations of fipronil and fipronil sulfone in eggs, liver, fat, and brain with experimental data from quail. Results showed that while the model could predict trends in fipronil distribution and metabolism, there were discrepancies in the peak concentration times (Tmax) of fipronil sulfone in liver and brain, and maximum concentrations (Cmax) of fipronil and fipronil sulfone in fat when compared to experimental data, particularly in the timing of fipronil sulfone accumulation. These findings underscore the need for further refinement of PBK models for avian species. However, they also highlight the potential for such models to reduce the reliance on animal testing in environmental risk assessments. The model developed here represents an important step towards a generic avian PBK model, which could be used for assessing the risks of various chemicals in different bird species. The findings of this study will guide future research in the development and refinement of PBK models for avian species, thereby contributing to the advancement of toxicology research.

Keywords: Physiologically based kinetic modeling; Fipronil; Fiprinil sulfone; Birds

1. Introduction

Physiologically-based kinetic (PBK) models have emerged as valuable tools in biomedical, pharmaceutical, and toxicology research, as well as in risk assessment (Krishnan & Peyret, 2009). These models consist of mathematical equations that describe how a compound is absorbed, distributed, metabolized, and excreted (ADME) within an organism, a process also known as toxicokinetics (Horak et al., 2018; Paini et al., 2019). Understanding toxicokinetics through PBK models can help estimate the internal dose from an external exposure concentration or, conversely, estimate the external exposure concentration from a known internal dose. This capability is crucial for predicting toxicity and can potentially replace traditional animal testing (US EPA, 2023). In PBK models, the organism is represented as a set of compartments corresponding to different organs and tissues, visualized as individual boxes. Each compartment is assumed to have a uniform xenobiotic concentration, and they are interconnected through the blood circulation system (Rietjens et al., 2011). PBK models simulate time-concentration curves of a chemical in each compartment, effectively predicting the biokinetics of drugs and

* Corresponding author.
E-mail address: thitirat.kanokjiraporn@wur.nl
Submission date: 19 August 2024
ECTS: 24
Word count: 5,174 words

chemicals in organisms without the need for in vivo experiments (Baier et al., 2022). Currently, assessing the environmental risks of xenobiotic substances often requires numerous animal tests across different species. However, as part of ongoing efforts to minimize animal testing, there is a push to use in silico methods, such as PBK models, to support risk assessment (Lilienblum et al., 2008). ('Regulation 1107/2009', n.d.) emphasizes that risk assessors should minimize the requirement for animal tests to determine the toxicity of chemicals across various species. The regulation advocates for the use of non-animal methods and prohibits the repetition of vertebrate studies. Despite this, very few non-animal test methods have been validated for regulatory toxicology. Specifically, no officially accepted non-animal methods currently exist for assessing chemical toxicity in birds for risk assessment purposes. Nonetheless, the European Food Safety Authority (EFSA) provides guidelines for conducting risk assessments for birds and mammals using non-animal toxicity data and suggests utilizing the PBK model as well (Authority (EFSA) et al., 2023). This highlights the importance of developing the PBK models for bird species.

Research by (Dogruer et al., 2021) highlights the benefits of using PBK models for the preservation of local species. They introduced a three-part framework that demonstrates how in silico and in vitro tests can be integrated to develop a comprehensive, mechanism-based chemical risk assessment. The process began with the creation and validation of a PBK model to understand the lifetime accumulation of cadmium in the kidneys of green sea turtles. This involved simulating chemical concentrations in the target organ for effect assessment. Next, a PBK-based quantitative in vitro to in vivo extrapolation (QIVIVE) was performed using reverse dosimetry PBK modeling and basal in vitro cytotoxicity data. This approach, commonly referred to as bottom-up PBK modeling, uses in vitro assay data to estimate in vivo exposure to a xenobiotic (Tan et al., 2018). QIVIVE has been used widely in the pharmaceutical sector for the prediction of drug-drug interactions, the modeling of systemic exposure in diseases, and the prediction of pharmacokinetics in special populations (Rowland et al., 2011; Shebley et al., 2018). The simulated internal concentration-response relationships were then validated using concentration-dependent health biomarkers. This led to the assessment of toxicity thresholds, including cytotoxicity thresholds at the biological target site, and the determination of the corresponding environmental threshold value. Finally, adverse health risks were quantified by comparing these threshold values to reported environmental concentrations, providing insight into the current risk of the chemical to the species of interest. Overall, this framework offers a simple and cost-effective method for predicting and proactively managing environmental issues. It can also be applied to models for different chemicals and species, helping to prioritize actions for addressing harmful long-term chemical exposures. For regulatory frameworks, the quantitatively derived exposure threshold limits for wildlife risk assessment facilitate the practical application of science-based policy decisions.

Significant progress has been made in developing PBK models for mammal species due to their applications in pharmacology. However, compared to mammals, the development of PBK models for birds, which are important in environmental risk assessment (e.g., for pesticides), is not as advanced (Mavroudis et al., 2018). Most available PBK models of birds are PBK models simulating veterinary drugs in chickens (Thompson et al., 2021). Apart from that, there are only a handful of PBK models developed to simulate specific chemicals in other bird species, for example, American kestrels, turkeys, pheasants, and quails (Cortright et al., 2009; Fernie et al., 2011). Typically, specific PBK models are adjusted to fit the kinetics of individual compounds. The development of such models necessitates extensive kinetic data to allow for thorough parameterization, precise calibration, and validation (Jongeneelen & Berge, 2011; Lu et al., 2016). Regrettably, such data are frequently unavailable for most non-pharmaceutical chemicals, which obstructs the use of PBK models for chemicals with limited data availability. As an alternative, a generic PBK approach can be employed. Generic PBK models have a predetermined compartmental structure with species-specific physiological parameters, and chemical-specific parameters can be derived from in vitro biokinetic metabolism assays combined with in silico models (Paini et al., 2019; Punt et al., 2022). The limited availability of PBK models for many bird species underlines the need for developing a generic avian PBK model covering bird species commonly used in environmental risk assessment, especially for plant protection products (PPP) given their widespread use, dispersal, and toxic potencies.

The application of PPP to protect crop yields from pests and diseases poses a risk to the ecosystem (Jeschke, 2016; Spaiser et al., 2017; UN General Assembly, 2015). These products disperse into the air, soil, surface water, groundwater, and oceans, leading to potentially adverse effects on non-target species including avian species (Fantke et al., 2012; Fantke & Jolliet, 2016; Halleux, 2023; Li, 2020)(Fantke et al., 2012; Fantke & Jolliet, 2016; Halleux, 2023; Li, 2020). They are exposed to PPPs through inhalation of contaminated air, dermal contact during and after spray application, and oral uptake via their food sources such as crops, weeds, and insects. Additionally, their feathers can come into contact with residue on crops and weeds (EFSA (European Food Safety Authority), 2009). This indicates that the use of PPPs potentially poses a significant threat to the health of bird populations. Therefore, proper risk assessments for PPPs in avian species are essential.

Fipronil is a pesticide widely used for plant protection and pest control on pets (Diepens et al., 2023; Ministerie van Landbouw, 2017). Fipronil potentially enters surface water via wastewater discharge from the washout and accumulates in the environment due to its persistence in soil (Bhatt et al., 2023; Perkins et al., 2024). Birds can be exposed to fipronil via contaminated seed and the environment (Szabo et al., 2009). In 2017, it was discovered that some eggs had been contaminated with fipronil in the Netherlands, showing the potential to accumulate in the food chain (Corrias et al., 2021). Furthermore, the research highlighted differences in sensitivity to fipronil among bird species (*Fipronil Environmental Effects*, n.d.). This sensitivity varies widely from being highly toxic in Galliform birds (with LD50 values of 11.3, 31, and 34 mg/kg for bobwhite quail, ring-necked pheasant, and red-legged partridge, respectively) to being non-toxic in mallard ducks (with an LD50 value greater than 2,150 mg/kg) (US EPA, 1996). This variation complicates the ability to predict fipronil toxicity in avian species that have not been studied.

This study aims to develop a PBK model for the bobwhite quail (*Colinus virginianus*), adapted from an existing chicken (*Gallus gallus domesticus*) PBK model. The model was designed to simulate the pharmacokinetic profile of fipronil in quail, with a particular focus on its major metabolite, fipronil sulfone. The simulations were evaluated against existing experimental pharmacokinetic data in quail, specifically comparing the model's predictions with in vivo data of substrate concentration in liver, fat, and brain reported in the literature.

Abbreviations

AUC	Area under the curve
Cmax	Maximum concentration
Km	Michaelis-Menten constant
QIVIVE	Quantitative in vitro to in vivo extrapolation
PBK	Physiologically based kinetic
PPP	Plant protection product
Tmax	Corresponding time of maximum concentration
Vmax	Maximum rate achieved

2. Materials and methods

2.1. PBK model structure and development

The chicken model from (Lautz et al., 2022) consists of two sub-models, including fipronil as a parent compound and fipronil sulfone as a major metabolite. The structure of the model has eleven compartments, including the gut, liver, fat, brain, kidney, bone, muscle, lung, heart, reproductive system, and egg, connected by the circulatory system. The model structure for this study was simplified by grouping muscle and bone as slowly perfused tissue, while the lung, heart, and remaining tissues were grouped as rapid perfused tissue. Hence, the model structure of this study consists of nine compartments, including the gut, liver, fat, brain, kidney, rapidly perfused tissue, slowly perfused tissue, reproductive system, and egg, connected by the circulatory system. Oral intake was used as an exposure scenario, due to the in vivo data available on the result of substrate concentration in eggs for chicken and in liver, fat, and brain for quail after oral administration. The elimination processes, including hepatic metabolism, renal excretion, and transfer to the egg, were included in the model structure as well (Figure 1). There was no further conversion of the fipronil sulfone was detected from an in vitro incubation experiment by (Lautz et al., 2022). Available data also addressed that fipronil sulfone is very stable in chicken (Gerletti et al., 2020; Kitulagodage, 2011), so the clearance of fipronil sulfone was not included in this study. Mathematical equations were defined following the study from Lautz et al. (2022). Differential equations were implemented using Berkeley Madonna (Version 10.2.8; University of California at Berkeley, CA, USA). Graphical representations were carried out using GraphPad Prism version 10.0.0 for Windows (GraphPad Software, Boston, Massachusetts, USA).

The generic PBK model described in Lautz et al. (2022) and scripted in R, simulating the concentration-time profile of chemicals in chicken (*Gallus gallus domesticus*), was scripted in Berkeley Madonna (Version 10.2.8) in this study. Its performance was evaluated by the concentration of fipronil in the egg measured in vivo from MacLachlan (2008) (see section 2.3). Once the generic PBK model of chicken in Berkeley Madonna was evaluated, it was adjusted to model the concentration of fipronil and fipronil sulfone in quail by adjusting both the physiological and pharmacokinetic parameters in the model to describe the pharmacokinetics of the chemicals in quail (see section 3.2).

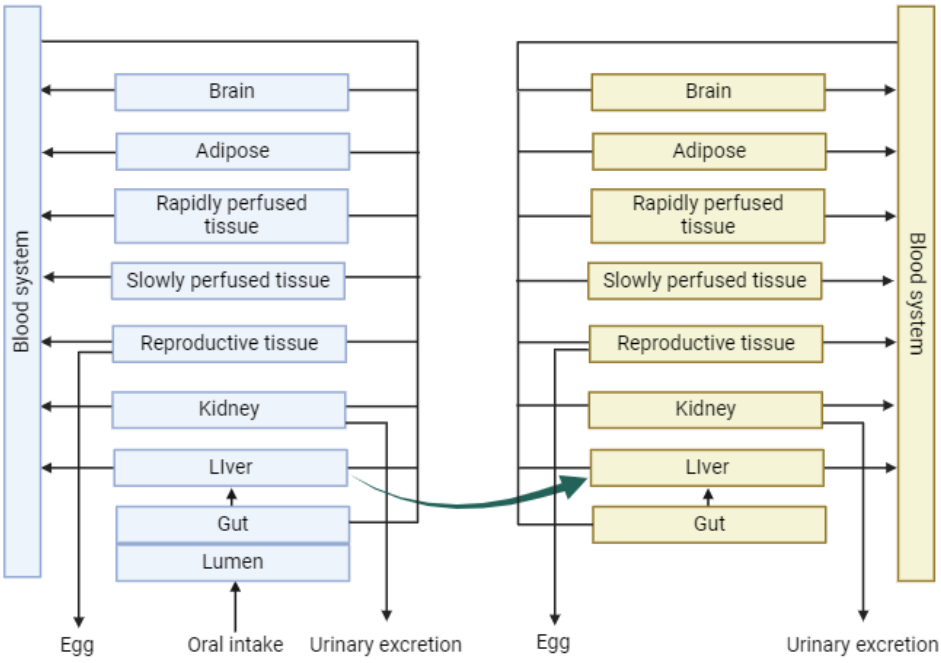

Figure 1. Structure of the PBK model for chicken and quail. Fipronil enters the body via oral intake and enters the general bloodstream from the gut lumen and through liver. On the left side is the pathway of fipronil, which is metabolised (green arrow) to fipronil sulfone in the liver, which then circulates the body as depicted in the flow diagram on right side. Fipronil and its metabolite are excreted via eggs and urine.

2.2. PBK model parameterization

Physiological parameters for chicken were obtained from (Lautz et al., 2020, 2022) (Table 1). Physicochemical parameters for the chicken PBK model in this study were obtained from (Lautz et al., 2020), while pharmacokinetic parameters for the chicken were obtained from (Lautz et al., 2022). Notable differences between the (Lautz et al., 2022) model and the chicken PBK model in this study are that there is no separate compartment for bone, muscle, lung, and heart. Apart from the main organs, muscle and bone were grouped as slowly perfused tissue, while the lung, heart, and remaining tissues were grouped as rapid perfused tissue.

The physiological parameters for the quail PBK model were gathered from various studies. Most of the physiological parameter values are from the study of bobwhite quail (*Colinus virginianus*) (Baier et al., 2022; Mahmoud & Coleman, 1967). However, some parameter values cannot be found for the same species, so they were gathered from the study of a close species, Japanese quail (*Coturnix japonica*) (Igado & Aina, 2010; Kawahara & Saito, 1976). As mentioned above, the fraction of slowly perfused tissue was calculated by combining muscle and bone tissue, while rapid perfused tissue was calculated by combining the lung, heart, and the remaining tissues. Michaelis-Menten kinetics parameters, including maximum reaction rate (Vmax) and Michaelis-Menten constant (Km), were achieved from the study on Japanese quail showing Vmax = 271 pmol/min/ mg protein and Km = 180 µM which resulted in hepatic intrinsic clearance (Vmax/Km) equal to 1.5 µL/min/mg protein. The fraction of blood flow and physicochemical parameters values for quail are not available; hence, the parameter values for chicken were used instead. A list of parameters and their values for both chicken and quail models and the reference are provided in Table 1.

Table 1. Physiological, physiochemical, and kinetic parameter values for the PBK model for chicken and quail.

Parameter	Abbreviation	Chicken	Reference	Quail	Reference
Physiological parameters					
Body weight; Kg	BW	2.11	Lautz et al. 2020	0.2	Baier et al. 2022
Fraction of fat tissue	VFc	0.107	Lautz et al. 2020	0.015	Baier et al. 2022
Fraction of liver tissue	VLc	0.024	Lautz et al. 2020	0.0135	Baier et al. 2022
Fraction of blood	VBc	0.071	Lautz et al. 2020	0.08	Baier et al. 2022
Fraction of rapid perfused tissue	VRc	0.109	Lautz et al. 2020	0.2599	Baier et al. 2022 (Calculated)
Fraction of slowly perfused tissue	VSc	0.611	Lautz et al. 2020	0.5809	Baier et al. 2022 (Calculated)
Fraction of brain tissue	VBRc	0.003	Lautz et al. 2020	0.00355	Igado. 2010
Fraction of gut tissue	VGc	0.039	Lautz et al. 2020	0.01505	Kawanara&Saito 1975
Fraction of reproductive tissue	VRPc	0.028	Lautz et al. 2020	0.0256	Kawanara&Saito. 1975
Fraction of kidney tissue	VKc	0.008	Lautz et al. 2020	0.0065	Baier et al. 2022
Volume of egg; Kg	VEgg	0.055	MacLachlan 2008	0.0104	Mahmoud&Colem an. 1967
Cardiac output; L/hr	QC	0.34*60*BW	Lautz et al. 2020	0.05*60*BW	Baier et al. 2022
Fraction of blood flow to fat tissue	QFc	0.015	Lautz et al. 2020	0.015	Lautz et al. 2020
Fraction of blood flow to liver tissue	QLc	0.066	Lautz et al. 2020	0.066	Lautz et al. 2020
Fraction of blood flow to brain tissue	QBRc	0.004	Lautz et al. 2020	0.004	Lautz et al. 2020
Fraction of blood flow to gut tissue	QGc	0.177	Lautz et al. 2020	0.177	Lautz et al. 2020
Fraction of blood flow to rapid perfused tissue	QRc	0.159	Lautz et al. 2020	0.159	Lautz et al. 2020
Fraction of blood flow to slowly perfused tissue	QSc	0.322	Lautz et al. 2020	0.322	Lautz et al. 2020
Fraction of blood flow to reproductive tissue	QRPc	0.143	Lautz et al. 2020	0.143	Lautz et al. 2020
Fraction of blood flow to kidney tissue	QKc	0.114	Lautz et al. 2020	0.114	Lautz et al. 2020
Blood flow to egg; L/hr	QEgg	0.012	Lautz et al. 2020	0.012	Lautz et al. 2020

Parameter	Abbreviation	Chicken	Reference	Quail	Reference
Physicochemical parameters					
Fat tissue/ blood partition coefficient of fipronil	PFfip	104	Lautz et al. 2020	104	Lautz et al. 2020
Liver tissue/ blood partition coefficient of fipronil	PLfip	8.12	Lautz et al. 2020	8.12	Lautz et al. 2020
Brain tissue/ blood partition coefficient of fipronil	PBRfip	12.98	Lautz et al. 2020	12.98	Lautz et al. 2020
Gut tissue/ blood partition coefficient of fipronil	PGfip	10.25	Lautz et al. 2020	10.25	Lautz et al. 2020
Rapid perfused tissue/ blood partition coefficient of fipronil	PRfip	3.21	Lautz et al. 2020	3.21	Lautz et al. 2020
Slowly perfused tissue/ blood partition coefficient of fipronil	PSfip	5.01	Lautz et al. 2020	5.01	Lautz et al. 2020
Reproductive tissue/ blood partition coefficient of fipronil	PRPfip	8.12	Lautz et al. 2020	8.12	Lautz et al. 2020
Kidney tissue/ blood partition coefficient of fipronil	PKfip	4.94	Lautz et al. 2020	4.94	Lautz et al. 2020
Fat tissue/ blood partition coefficient of fipronil-sulfone	Pfsul	117	Lautz et al. 2020	117	Lautz et al. 2020
Liver tissue/ blood partition coefficient of fipronil-sulfone	Plsul	8.34	Lautz et al. 2020	8.34	Lautz et al. 2020
Brain tissue/ blood partition coefficient of fipronil-sulfone	PBRsul	13.3	Lautz et al. 2020	13.3	Lautz et al. 2020
Gut tissue/ blood partition coefficient of fipronil-sulfone	Pgsul	10.5	Lautz et al. 2020	10.5	Lautz et al. 2020
Rapid perfused tissue/ blood partition coefficient of fipronil-sulfone	Prsul	3.29	Lautz et al. 2020	3.29	Lautz et al. 2020
Slowly perfused tissue/ blood partition coefficient of fipronil-sulfone	Pssul	5.14	Lautz et al. 2020	5.14	Lautz et al. 2020
Reproductive tissue/ blood partition coefficient of fipronil-sulfone	PRPsul	8.34	Lautz et al. 2020	8.34	Lautz et al. 2020
Kidney tissue/ blood partition coefficient of fipronil-sulfone	Pksul	5.1	Lautz et al. 2020	5.1	Lautz et al. 2020
Pharmacokinetic parameters					
Fraction of absorption	fa	0.5	Lautz et al. 2022	0.5	Lautz et al. 2022
Absorption constant; /hr	ka	0.6	Lautz et al. 2022	0.6	Lautz et al. 2022
S9 protein yield per wet weight liver; mg/g	MPL	60	Lautz et al. 2022	60	Lautz et al. 2022
Fipronil hepatic intrinsic clearance; ul/min/mg	cl_fip	29.6	Lautz et al. 2022	1.5	(Khidkhan et al., 2022)
Fipronil renal clearance; L/min/kg	cl_renal	0	Lautz et al. 2020	0	Lautz et al. 2020

2.3. Model evaluation and sensitivity analysis

The PBK model was validated by comparing the model prediction and in vivo data of fipronil and fipronil sulfone concentration within the organs, which were obtained from the literature. Fipronil concentration in eggs (D. j. MacLachlan, 2008) were used for chicken model validation, while fipronil and its metabolite concentrations in liver, fat, and brain (Kitulagodage, 2011) were used for quail model validation, according to the data available.

Sensitivity analysis is a methodical investigation that helps understand how changes in a model's input parameters can impact its simulation outputs (Pletz et al., 2020). It involves changing each parameter one by one while keeping the others constant. The normalized sensitivity coefficients (SC) are then calculated using the following formula (Eq. 1).

$$SC = \frac{(C' - C)}{(P' - P)} \times \frac{P}{C} \tag{1}$$

Here, C represents the initial value of the model output, C' represents the output after a 1% parameter change, P represents the initial parameter value, and P' represents the parameter value modified by an increase of 1%. This formula helps quantify the degree to which changes in each parameter affect the model output (Chiu et al., 2007; Strikwold et al., 2013). The parameters with an absolute SC value higher than 0.1 are considered as significantly affected (Rietjens et al., 2011).

3. Results

The aim of this study was to develop a PBK model for simulating tissue concentrations of the pesticide fipronil and its metabolite, fipronil sulfone, in quail based on a generic PBK model for chicken. Predicting quantities such as the area under the curve (AUC) or maximum concentration (Cmax) and corresponding times (Tmax) after oral exposure were performed by the developed quail model. The structure of the generic PBK model is illustrated in Figure 1, and Appendix A.1 and A.2 provide code of the PBK model for both chicken and quail.

3.1. Chicken model

The case study that was used as a validation gave 0.103 mg/kg BW of fipronil for chicken, resulting in a slight increase in fipronil concentration in eggs and level off at 0.0918 mg/kg from day 20 to day 42 (MacLachlan, 2008). As shown in Figure 2, the prediction from the chicken PBK model underestimated the maximum concentration in the egg by 230-fold. Moreover, the duration of concentration accumulation until reaching the peak is much sooner compared to the in vivo data (Table 2).

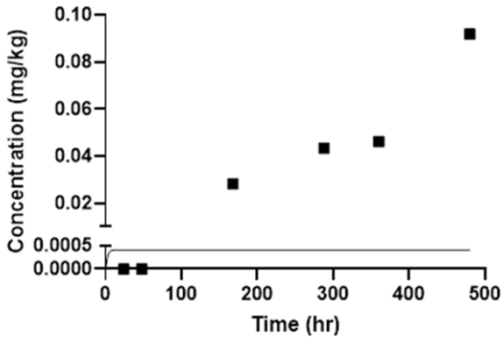

Figure 2. Comparison of the concentration of fipronil in the egg predicted by a chicken model (solid line) and the concentration of fipronil in the egg measured *in vivo* from (MacLachlan, 2008) at an oral dose of fipronil 0.103 mg/kg BW exposure (filled square).

Table 2. The area under curve (AUC), maximum concentration (Cmax), and corresponding times (Tmax) of fipronil concentration from chicken model prediction and *in vivo* data (MacLachlan, 2008).

	Model prediction	*In vivo* data
AUC	0.1924	17.4700
Cmax	0.0004	0.0918
Tmax	13.05	480.00

3.2. Quail model

The study from Kitulagodage et al. (2011) showed the consistency concentrations from hour 8 to hour 96 showed that fipronil concentrations in the liver and brain were metabolized rapidly. Fipronil possibly turned into its metabolite, fipronil sulfone, within the first 8 hours. This aligns with the model prediction, which showed the peak within the first 8 hours, then sharply decreased and leveled off (Figure 3A and 3C). While measured fipronil sulfone concentration in the liver and brain from the study of Kitulagodage et al. (2011) gradually increased and reached the peak (Cmax = 22.33 and 10.23 mg/kg in liver and brain, respectively) at hour 72 (Table 4). This contrasts with the model prediction, which states that the fipronil sulfone concentration sharply increases during the first 8 hours in the liver, resulting in a large difference in Tmax. However, the Cmax of the fipronil sulfone prediction is similar to the measured data, resulting in a 1.36-fold difference (Figure 3D and Table 4). The trend of measured fipronil sulfone concentration in brain is similar to the one in liver but lower in amount of substrate (Kitulagodage et al., 2011). Therefore, the model prediction of fipronil sulfone concentration in the brain has a much lower Cmax compared to the in vivo data, around 14.9-fold (Figure 3F and Table 4).

Fipronil and its metabolite concentrations are most concentrated in fat tissue, according to the lipophilic characteristics of fipronil and fipronil sulfone (log Kow = 4.0 and 4.42, respectively (Kim et al., 2021; Lautz et al., 2022) (Figures 3B and 3E). However, the model prediction of fipronil and fipronil sulfone concentrations is much lower than the measured data, resulting in 226.6-fold and 277.0-fold differences, respectively (Tables 3 and 4).

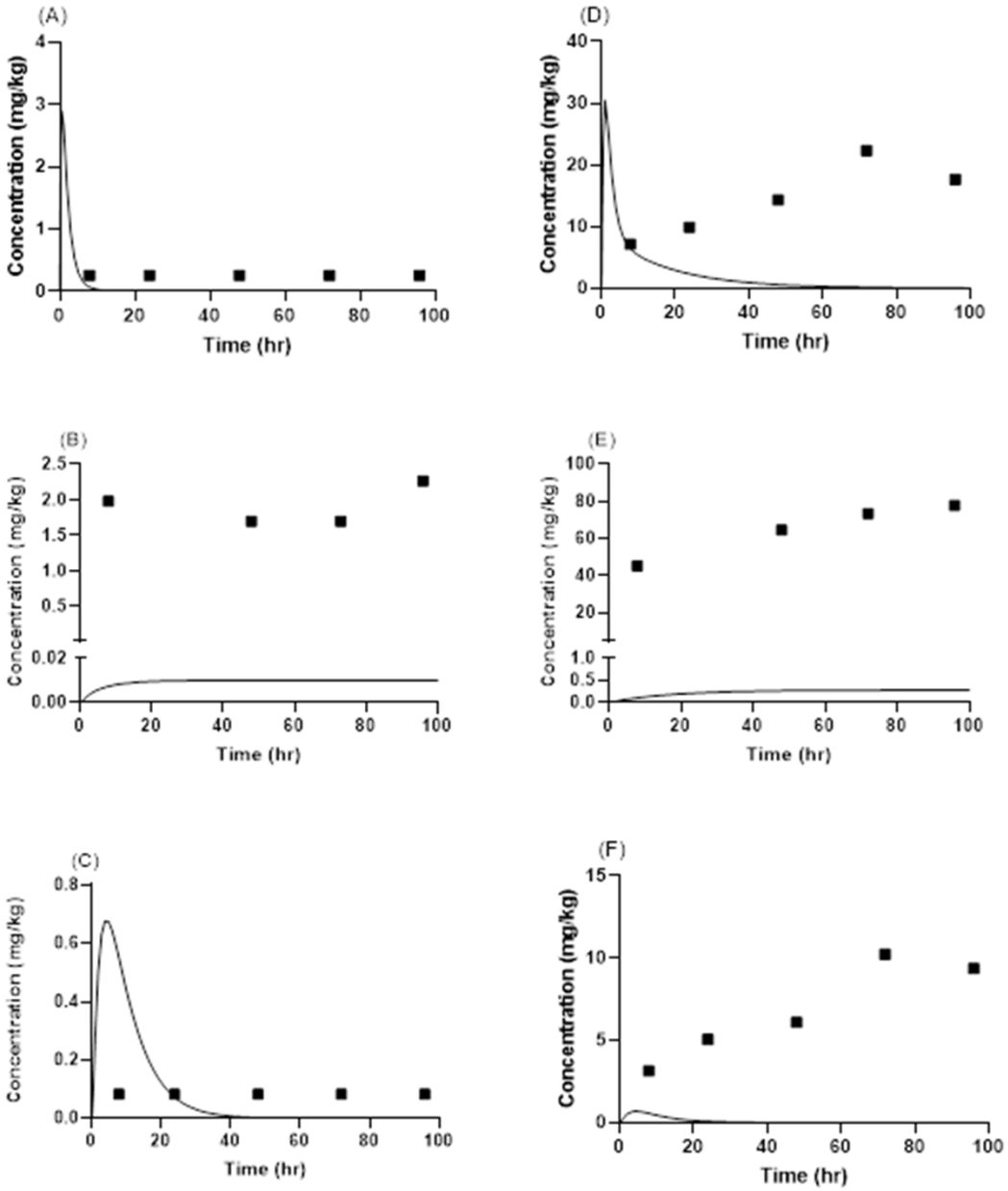

Figure 3. Comparison of the concentration of fipronil in liver (A), fat (B), and brain (C) and concentration of fipronil sulfone in liver (D), fat (E), and brain (F) predicted by a quail model (solid line) and the concentration of fipronil in the measured *in vivo* from (Kitulagodage et al., 2011) at an oral dose of fipronil 11.3 mg/kg BW exposure (filled square).

Table 3. The area under curve (AUC), maximum concentration (Cmax), and corresponding times (Tmax) of fipronil concentration from quail model prediction and *in vivo* data (Kitulagodage et al., 2011).

Fipronil	Liver		Fat		Brain	
	Model prediction	*In vivo* data	Model prediction	*In vivo* data	Model prediction	*In vivo* data
AUC	7.525	22.5	0.9379	161.8	8.697	7.293
Cmax	2.891	0.2557	0.01	2.266	0.6779	0.08287
Tmax	0.5243	7.914	44.91	95.91	3.914	7.914

Table 4. The area under curve (AUC), maximum concentration (Cmax), and corresponding times (Tmax) of fipronil sulfone concentration from quail model prediction and *in vivo* data (Kitulagodage et al., 2011).

Fipronil	Liver		Fat		Brain	
	Model prediction	*In vivo* data	Model prediction	*In vivo* data	Model prediction	*In vivo* data
AUC	220	1346	23.46	77.9	8.911	630.5
Cmax	30.48	22.33	0.2812	77.9	0.6855	10.23
Tmax	1.049	71.91	100	95.91	3.914	71.91

3.3. Sensitivity analysis

A sensitivity analysis was conducted on each parameter individually to observe how small perturbations (1%) from the parameter values (x-axis) impact the model prediction and influence the output (in this case Cmax and AUC). The parameters with an absolute SC value higher than 0.1 were shown here since they were considered significantly affected (Rietjens et al., 2011). The higher the sensitivity index for a parameter, the greater the impact on the output (Figure 4).

The fraction of absorption has a high influence on all model predictions. The parameters related to the liver, including VLc, MPL, and fipronil hepatic intrinsic clearance have a high influence on both Cmax and AUC of fipronil concentration in all three types of tissue, including liver, fat, and brain, but it does not much influence fipronil sulfone concentration prediction except for the concentration in the brain. Most of the parameters, especially for the fraction of blood flow to the tissues, have a strong influence on AUC over Cmax (Figure 4D). While each of the parameters influences Cmax and AUC differently, the result in fat tissue shows the similarity in the level of parameter influences Cmax and AUC (Figure 4B and 4E). This is related to the trend of model prediction on fipronil and fipronil sulfone concentration in fat (Figures 3B and 3E).

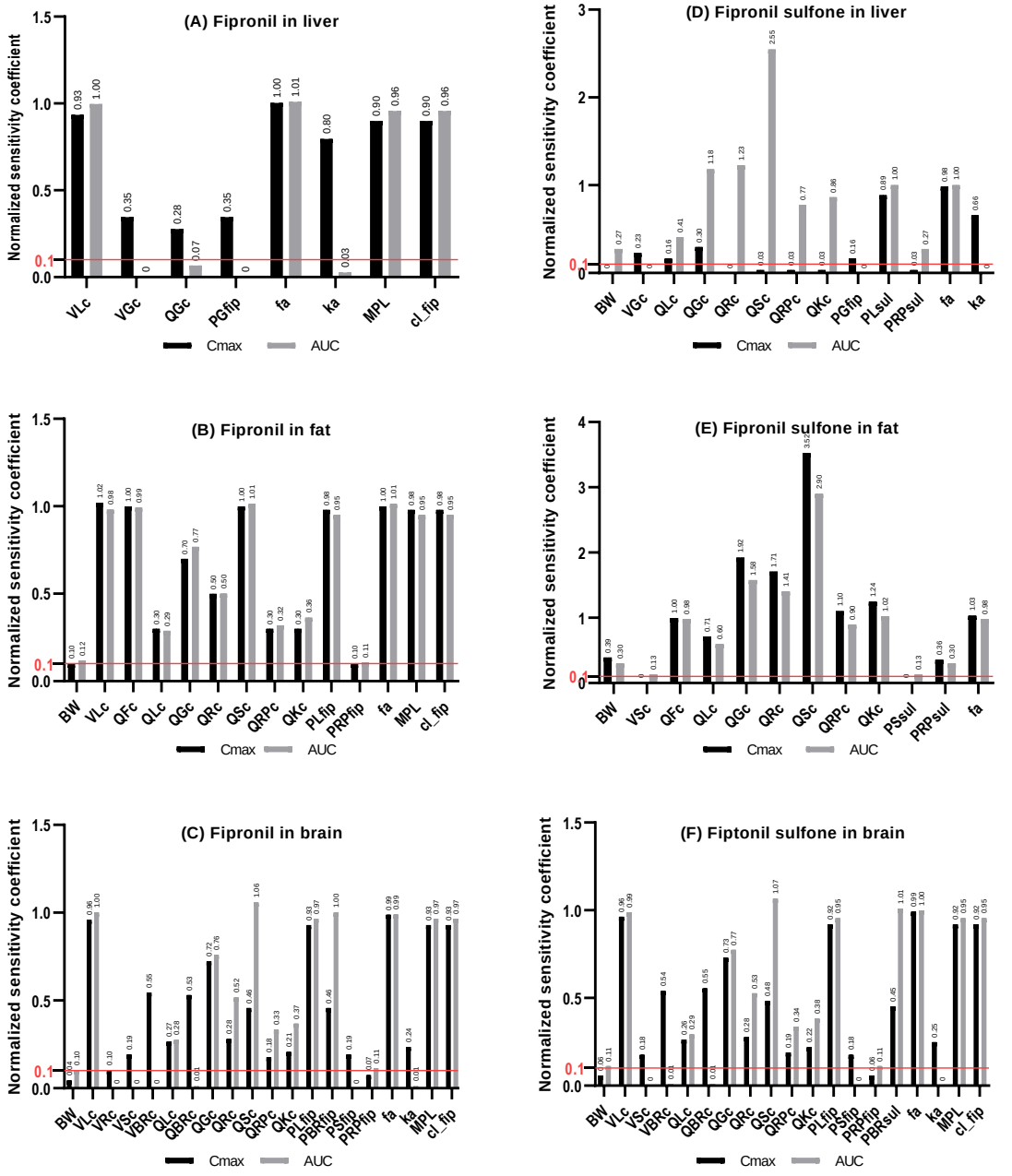

Figure 4. Comparison of the normalized sensitivity coefficient of various parameters derived from the model's predictions on the maximum concentration (Cmax: black bar) and the area under curve (AUC: gray bar) of fipronil concentration in the liver (A), fat (B), and brain (C) and fipronil sulfone concentration in the liver (D), fat (E), and brain (F). The sensitivities for the quail on a dose of 11.3 mg fipronil/kg BW. Each bar indicates the normalized sensitivity coefficient of a particular parameter, with the absolute value of the coefficient showing how the parameter influences the model output. Parameters with absolute values exceeding 0.1 (red solid line) were shown here since they are considered significant influences (Rietjens et al., 2011). The parameters stand for BW= body weight, VLc= fraction of liver tissue, VSc= fraction of slowly perfused tissue, VBRc= fraction of brain tissue, VGc= fraction of gut tissue, QFc = fraction of blood flow to fat, QLc= fraction of blood flow to liver, QBRc= fraction of blood flow to brain, QGc= fraction of blood flow to gut, QRc= fraction of blood flow to rapid perfused tissue, QSc= fraction of blood flow to slowly perfused tissue, QRPc= fraction of blood flow to reproductive tissue, QKc= fraction of blood flow to kidney, PLfip= liver/blood partition coefficient of fipronil, PBRfip= brain/blood partition coefficient of fipronil, PGfip= gut/blood partition coefficient of fipronil, PSfip= slowly perfused tissue/blood partition coefficient of fipronil, PRPfip= reproductive tissue/blood partition coefficient of fipronil, PLsul= liver/blood partition coefficient of fipronil sulfone, PSsul= slowly perfused tissue/blood partition coefficient of fipronil, PRPsul= reproductive tissue/blood partition coefficient of fipronil, fa= fraction of absorption, ka= absorption constant, MPL= S9 protein yield per gram wet weight liver, and cl_fip= fipronil hepatic intrinsic clearance.

4. Discussion

4.1. Model Evaluation and Sensitivity Analysis

The prediction from the recreated chicken PBK model was not as we expected due to the over 10-fold difference in the prediction. Even though most of the parameters and mathematical equations were gathered from the same study, it gave a totally different result compared to the in vivo data and also the prediction itself from the original study. This indicates a hole in translating the code from R software into Berkeley Madonna, especially for the exposure scenario, which is not clearly shown in the code, which might cause the mistranslation.

Based on the quail model prediction, further validation of the model is necessary. The sensitivity analysis results indicate that certain parameters strongly influence the model's prediction, and adjusting their values would aid in model validation. The absorption fraction used in this study is 0.5, as recommended by Lautz et al. (2022). However, this value could vary from 0.44 to 0.72 (Gerletti et al., 2020; Kitulagodage, 2011). Additionally, studies by Khidkhan et al. (2022) and Lautz et al. (2022) reported different values of fipronil hepatic intrinsic clearances of 6.4 and 29.6 ul/min/mg protein, respectively. The prediction of both fipronil and fipronil sulfone concentration from quail model, especially in liver and brain, reached the peak of concentration sooner than the actual concentration from the in vivo study (Tmax of the model prediction is lower than the one from in vivo data) and also eliminated faster. This might align with the kinetic parameter values as well. The accuracy of the PBK model might be affected due to interspecies differences since the parameters used to develop the model were gathered from different species. PBK model equations were based on chicken, while some data were collected from close species available in the literature, the Japanese quail (*Coturnix japonica*), or chicken data in case of there is no data available for quail.

4.2. Limitations and Recommendations

The chicken model, which was recreated based on an existing model, should be performed as well as the reference one. This is an initial step to further develop the quail model later on. However, the chicken model did not perform as well as we expected due to the time restriction. In order to improve that comparing with other generic chicken models should be considered. Apart from the generic chicken model from Baier et al. (2022) and Lautz et al. (2020) also develop a generic avian model on PK-Sim, which is able to predict the concentration in eggs as well. However, since these two models were developed on different platforms, similar to the one that was developed in this study, there is a loss of translation across the platform that should be considered as well. Moreover, the generic chicken model also was tested on many chemicals, so it should be considered to investigate as well in order to compare the prediction and improve the model for better prediction.

Acknowledgements

I want to express my deep gratitude to my supervisor, Nynke Kramer, for providing me with generous guidance and kind support, even though I have many restricted conditions regarding time and course that I have to complete during this research practice. I would also like to thank Nico van den Brink for giving me the opportunity to do research practice in the toxicology group again and for giving me good advice on this exciting topic that I am keen to further study in this topic in the future.

Appendix A. Berkley Madonna Code for fipronil and fipronil sulfone

A.1. Chicken model

```
;Date:23-07-2024
;Chemical: Fipronil
;Specie: Chicken
;Exposure: Single oral dose {mg/kg}
;Complied by: Thitirat Kanokjiraporn
;Organisation: Wageningen University

;=============================================================================
;Physiological parameters
;=============================================================================
```

```
;tissue volume
BW=2.11 {Kg}          ;body weight (Lautz et al. 2020=2.11) (Baier et al. 2022 = 1.36 kg) (MacLachlan
2008 = 1.6)
;fraction of tissue (Lautz et al. 2020)
VFc=0.107     ;fraction of fat tissue
VLc=0.024     ;fraction of liver tissue
VBc= 0.071    ;fraction of blood
VRc= 0.109    ;fraction of rapid perfused tissue  (Heart + Lung+etc)
VSc= 0.611    ;fraction of slowly perfused tissue (Muscle + Bone)
VBRc=0.003    ;fraction of brain tissue
VGc=0.039     ;fraction of gut tissue
VRPc=0.028    ;fraction of reproductive tissue
VKc=0.008     ;fraction of kidney tissue


VF = VFc*BW                {Kg}     ; volume of fat tissue (calculated)
VL = VLc*BW                {Kg}     ; volume of liver tissue (calculated)
VB = VBc*BW                {Kg}     ; volume of blood (calculated)
VR = VRc*BW                {Kg}     ; volume of rapid perfused tissue (calculated)
VS = VSc*BW                {Kg}     ; volume of slowly perfused tissue (calculated)
VBR = VBRc*BW      {Kg}     ; volume of brain (calculated)
VG = VGc*BW                {Kg}     ; volume of gut (calculated)
VRP = VRPc*BW       {Kg}    ; volume of reproductive (calculated)
VK = VKc*BW                {Kg}     ; volume of kidney (calculated)
VEgg = 0.055               {Kg}     ; 55g (MacLachlan 2008)



;-------------------------------------------------------------------------------------------------------------------
;blood flow rates
; reference: (Lautz et al. 2020)
QC = 0.34*60*BW      {L/hr}   ; cardiac output
QFc = 0.015          ; fraction of blood flow to fat
QLc = 0.066          ; fraction of blood flow to liver
QBRc = 0.004         ; fraction of blood flow to brain
QGc = 0.177          ; fraction of blood flow to gut
QRc = 0.159          ; fraction of blood flow to rapid perfused tissue
QSc = 0.322          ; fraction of blood flow to slowly perfused tissue
QRPc=0.143           ;fraction of blood flow to reproductive tissue
QKc=0.114            ;fraction of blood flow to kidney tissue

                     ;Total fractions is 1

QF = QFc*VF          {L/hr}   ; blood flow to fat tissue (calculated)
QL = QLc*QC                {L/hr}   ; blood flow to liver tissue (calculated)
QBR = QBRc*QC        {L/hr}   ; blood flow to brain tissue (calculated)
QG = QGc*QC                {L/hr}   ; blood flow to gut tissue (calculated)
QS = QSc*QC                {L/hr}   ; blood flow to slowly perfused tissue (calculated)
QR = QRc*QC                {L/hr}   ; blood flow to rapid perfused tissue (calculated)
QRP = QRPc*QC        {L/hr}   ; blood flow to reproductive tissue (calculated)
QK = QKc*QC                {L/hr}   ; blood flow to slowly kidney tissue (calculated)
QEgg = 0.012         {L/hr}   ; blood flow to egg (Lautz et al. 2020)


;=====================================================================
;Physicochemical parameters
;=====================================================================
```

```
;partition coefficients fipronil
;ref (Lautz et al. 2020)
PFfip = 104     ; fat/blood partition coefficient
PLfip = 8.12    ; liver/blood partition coefficient
PBRfip=12.98 ; brain/blood partition coefficient
PGfip=10.25   ;gut/blood partition coefficient
PRfip = 3.21    ; richly perfused tissue/blood partition coefficient (heart3.21, lung1.17)
PSfip = 5.01    ; slowly perfused tissue/blood partition coefficient (bone14.16, muscle5.01)
PRPfip=8.12   ;reproductive/blood partition coefficient
PKfip=4.94     ;kidney/blood partition coefficient


;-----------------------------------------------------------------------------------------------------------

;partition coefficients fipronil-sulfone
;ref (Lautz et al. 2020)

PFsul = 117     ; fat/blood partition coefficient
PLsul = 8.34    ; liver/blood partition coefficient
PBRsul=13.3   ; brain/blood partition coefficient
PGsul=10.5     ;gut/blood partition coefficient
PRsul = 3.29    ; richly perfused tissue/blood partition coefficient (heart3.29, lung1.19)
PSsul = 5.14    ; slowly perfused tissue/blood partition coefficient (bone14.54, muscle5.14)
PRPsul=8.34   ;reproductive/blood partition coefficient
PKsul=5.1      ;kidney/blood partition coefficient
;=====================================================================
;Kinetic parameters
;=====================================================================
;fa=Fractional absorption
fa=0.5                  ; fraction of absorption (Lautz et al. 2020=0.5)(MacLachlan 2008=0.74)

; Absorption constant
Ka  = 0.6           {/hr}   ;  (Lautz et al. 2022 :=0.01 {/min})

;Metabolism liver
MPL=60  ; (mg protein/g liver) scaling factor of liver  (Lautz et al. 2022)

;=====================================================================
;Run settings
;=====================================================================

;Molecular weight
MWfip = 437.1           ; Molecular weight fipronil (https://pubchem.ncbi.nlm.nih.gov/compound/Fipronil)
MWsul = 453.1           ; Molecular weight fipronil-sulfone
(https://pubchem.ncbi.nlm.nih.gov/compound/Fipronil-sulfone)

cl_fip1 = 29.6   {ul/min/mg s9 protein}    ;cl_fip= fipronil intrinsic clearance
cl_fip = cl_fip1*MPL*60*10E-6*VL*1000           {L/hr}
cl_renal = 0



;Oral dose
ODOSE1 = 0.103 {mg/kg BW}  ;(MacLachlan 2008 = 0.103)  (Corrias et al. 2021=11.63)

;feed 100g/d for 7 days (Corrias et al. 2021)

ODOSEmg = ODOSE1*BW
```

```
;time
Starttime = 0   ; in hr
Stoptime = 700          ; in hr

;====================================================================
;Model calculations
;====================================================================
; fipronil
CGfip = AGfip/VG
CVGfip = CGfip/PGfip
CLfip = ALfip/VL
CVLfip = CLfip/PLfip
mfs=cl_fip*CLfip
CFfip = AFfip/VF
CVFfip = CFfip/PFfip
CBRfip = ABRfip/VBR
CVBRfip = CBRfip/PBRfip
CRfip = ARfip/VR
CVRfip = CRfip/PRfip
CSfip = ASfip/VS
CVSfip = CSfip/PSfip
CKfip = AKfip/VK
CVKfip = CKfip/PKfip
Urine1= cl_renal* CKfip
CRPfip = ARPfip/VRP
CVRPfip = CRPfip/PRPfip
Egg1 = QEgg * CRPfip
CV1 = (QF*CVFfip + (QG+QL)*CVLfip + QBR*CVBRfip + QR*CVRfip + QS*CVSfip + QK*CVKfip +
QRP*CVRPfip)/QC
CA1 = ABfip/VB
CEggfip = AEgg1/VEgg

;fipronil sulfone
CGsul = AGsul/VG
CVGsul = CGsul/PGsul
CLsul = ALsul/VL
CVLsul = CLsul/PLsul
CFsul = AFsul/VF
CVFsul = CFsul/PFsul
CBRsul = ABRsul/VBR
CVBRsul = CBRsul/PBRsul
CRsul = ARsul/VR
CVRsul = CRsul/PRsul
CSsul = ASsul/VS
CVSsul = CSsul/PSsul
CKsul = AKsul/VK
CVKsul = CKsul/PKsul
CRPsul = ARPsul/VRP
CVRPsul = CRPsul/PRPsul
Egg2 = QEgg * CRPsul
C_Egg=AEgg2/0.0011875
Egg_ex=C_Egg*0.002375
CV2 = (QF*CVFsul + (QG+QL)*CVLsul + QBR*CVBRsul + QR*CVRsul + QS*CVSsul + QK*CVKsul +
QRP*CVRPsul)/QC
CA2 = ABsul/VB
```

```
;fipronil (diff)
Alu' = -Ka* Alu          Init Alu = ODOSEmg*fa
Absorb1' = Ka * Alu      Init Absorb1 = 0
AGfip' = QG*(CA1-CVGfip) + Ka *Alu              Init AGfip = 0
ALfip' = QL*(CA1-CVLfip) + QG*(CVGfip-CVLfip) - mfs                    Init ALfip = 0
Ameta' = mfs                    Init Ameta = 0
AFfip' = QF*(CA1-CVFfip)                Init AFfip = 0
ABRfip' = QBR*(CA1-CVBRfip)          Init ABRfip = 0
ARfip' = QR*(CA1-CVRfip)      Init ARfip = 0
ASfip' = QS*(CA1-CVSfip)                Init ASfip = 0
AKfip' = QK*(CA1-CVKfip)      -Urine1           Init AKfip = 0
AUrine1' = Urine1               Init AUrine1 = 0
ARPfip' = QRP*(CA1-CVRPfip)-Egg1    Init ARPfip = 0
AEgg1' = Egg1                           Init AEgg1 =0
ABfip' = QC*(CV1-CA1)          Init ABfip =0
MassBal1' = Absorb1-
(Ameta+AGfip+ALfip+AFfip+ARfip+ASfip+AKfip+AUrine1+ARPfip+AEgg1+ABfip)
Init MassBal1 = 0

Totalfri = Absorb1
Calculatedfri = (Ameta+AGfip+ALfip+AFfip+ARfip+ASfip+AKfip+AUrine1+ARPfip+AEgg1+ABfip)
ERRORfri=(Totalfri-Calculatedfri)/(Totalfri+1E-30)*100
MBfri=Totalfri-Calculatedfri + 1


;fipronil sulfone (diff)
AGsul' = QG*(CA2-CVGsul)                                Init AGsul = 0
ALsul' = QL*(CA2-CVLsul) + QG*(CVGsul-CVLsul) + mfs                    Init ALsul = 0
Amfs' = mfs                     Init Amfs = 0
AFsul' = QF*(CA2-CVFsul)                Init AFsul = 0
ABRsul' = QBR*(CA1-CVBRsul)          Init ABRsul = 0
ARsul' = QR*(CA2-CVRsul)      Init ARsul = 0
ASsul' = QS*(CA2-CVSsul)                Init ASsul = 0
AKsul' = QK*(CA2-CVKsul)                Init AKsul = 0
ARPsul' = QRP*(CA2-CVRPsul)-Egg2    Init ARPsul = 0
AEgg2' = Egg2-Egg_ex                    Init AEgg2 =0
AEgg3' = Egg_ex                         Init AEgg3 = 0
ABsul' = QC*(CV2-CA2)          Init ABsul =0
MassBal2' = Amfs-(AGsul+ALsul+AFsul+ARsul+ASsul+AKsul+ARPsul+AEgg2+AEgg3+ABsul)
Init MassBal2 = 0
```

A.2. Quail model

```
;Date:23-07-2024
;Chemical: Fipronil
;Specie: Bobwhite Quail
;Exposure: Single oral dose {mg/kg}
;Complied by: Thitirat Kanokjiraporn
;Organisation: Wageningen University

;=====================================================================
;Physiological parameters
;=====================================================================
;tissue volume
BW=0.2 {Kg} ;body weight (Khidkhan et al. 2022= 0.15-0.2 kg) (Baier et al. 2022 = 0.2 kg)
;fraction of tissue (Lautz et al. 2020)
VFc=0.015     ;fraction of fat tissue
VLc=0.0135    ;fraction of liver tissue
VBc= 0.08     ;fraction of blood
VRc= 0.2599   ;fraction of rapid perfused tissue  (Heart + Lung+etc)
VSc= 0.5809   ;fraction of slowly perfused tissue (Muscle + Bone)
VBRc=0.00355          ;fraction of brain tissue
VGc=0.01505 ;fraction of gut tissue
VRPc=0.0256 ;fraction of reproductive tissue
VKc=0.0065    ;fraction of kidney tissue


VF = VFc*BW                 {Kg}    ; volume of fat tissue (calculated)
VL = VLc*BW                 {Kg}    ; volume of liver tissue (calculated)
VB = VBc*BW                 {Kg}    ; volume of blood (calculated)
VR = VRc*BW                 {Kg}    ; volume of rapid perfused tissue (calculated)
VS = VSc*BW                 {Kg}    ; volume of slowly perfused tissue (calculated)
VBR = VBRc*BW       {Kg}    ; volume of brain (calculated)
VG = VGc*BW                 {Kg}    ; volume of gut (calculated)
VRP = VRPc*BW       {Kg}    ; volume of reproductive (calculated)
VK = VKc*BW                 {Kg}    ; volume of kidney (calculated)
VEgg = 0.0104                       {Kg}    ; 10.4g (Mahmoud&Coleman. 1967)



;---------------------------------------------------------------------------------------------------------------------
;blood flow rates
; reference: (Lautz et al. 2020)
QC = 0.05*60*BW       {L/hr}   ; cardiac output(Baier et al. 2022)
QFc = 0.015           ; fraction of blood flow to fat
QLc = 0.066           ; fraction of blood flow to liver
QBRc = 0.004          ; fraction of blood flow to brain
QGc = 0.177           ; fraction of blood flow to gut
QRc = 0.159           ; fraction of blood flow to rapid perfused tissue
QSc = 0.322           ; fraction of blood flow to slowly perfused tissue
QRPc=0.143            ;fraction of blood flow to reproductive tissue
QKc=0.114             ;fraction of blood flow to kidney tissue

                      ;Total fractions is 1

QF = QFc*VF           {L/hr}   ; blood flow to fat tissue (calculated)
QL = QLc*QC                 {L/hr}   ; blood flow to liver tissue (calculated)
QBR = QBRc*QC         {L/hr}   ; blood flow to brain tissue (calculated)
```

```
QG = QGc*QC                 {L/hr}   ; blood flow to gut tissue (calculated)
QS = QSc*QC                 {L/hr}   ; blood flow to slowly perfused tissue (calculated)
QR = QRc*QC                 {L/hr}   ; blood flow to rapid perfused tissue (calculated)
QRP = QRPc*QC       {L/hr}   ; blood flow to reproductive tissue (calculated)
QK = QKc*QC                 {L/hr}   ; blood flow to slowly kidney tissue (calculated)
QEgg = 0.012        {L/hr}   ; blood flow to egg (Lautz et al. 2020)


;====================================================================
;Physicochemical parameters
;====================================================================

;partition coefficients fipronil
;ref (Lautz et al. 2020)
PFfip = 104    ; fat/blood partition coefficient
PLfip = 8.12   ; liver/blood partition coefficient
PBRfip=12.98 ; brain/blood partition coefficient
PGfip=10.25   ;gut/blood partition coefficient
PRfip = 3.21   ; rapid perfused tissue/blood partition coefficient (heart3.21, lung1.17)
PSfip = 5.01   ; slowly perfused tissue/blood partition coefficient (bone14.16, muscle5.01)
PRPfip=8.12   ;reproductive/blood partition coefficient
PKfip=4.94    ;kidney/blood partition coefficient


;--------------------------------------------------------------------------------------------------------------------

;partition coefficients fipronil-sulfone
;ref (Lautz et al. 2020)

PFsul = 117    ; fat/blood partition coefficient
PLsul = 8.34   ; liver/blood partition coefficient
PBRsul=13.3  ; brain/blood partition coefficient
PGsul=10.5    ;gut/blood partition coefficient
PRsul = 3.29   ; richly perfused tissue/blood partition coefficient (heart3.29, lung1.19)
PSsul = 5.14   ; slowly perfused tissue/blood partition coefficient (bone14.54, muscle5.14)
PRPsul=8.34   ;reproductive/blood partition coefficient
PKsul=5.1      ;kidney/blood partition coefficient
;====================================================================
;Kinetic parameters
;====================================================================
;fa=Fractional absorption
fa=0.5                ; fraction of absorption (Lautz et al. 2022)

; Absorption constant
Ka  = 0.6          {/hr}   ;  (Lautz et al. 2022 :=0.01 {/min})

;Metabolism liver
MPL=60  ; (mg protein/g liver) scaling factor of liver  (Lautz et al. 2022)


;====================================================================
;Run settings
;====================================================================

;Molecular weight
MWfip = 437.1          ; Molecular weight fipronil (https://pubchem.ncbi.nlm.nih.gov/compound/Fipronil)
MWsul = 453.1          ; Molecular weight fipronil-sulfone
(https://pubchem.ncbi.nlm.nih.gov/compound/Fipronil-sulfone)
```

```
cl_fip1 = 1.5     {ul/min/mg protein}
;cl_fip= fipronil intrinsic clearance (Vmax/Km) (Khidkhan et al. 2022)
cl_fip = cl_fip1*MPL*60*10E-6*VL*1000          {L/hr}
cl_renal = 0



;Oral dose
ODOSE1 = 11.3 {mg/kg BW}    ;(Kitulagodage et al.2010)
ODOSEmg = ODOSE1*BW       {mg}


;time
Starttime = 0   ; in hr
Stoptime = 700          ; in hr

;=====================================================================
;Model calculations
;=====================================================================
; fipronil
CGfip = AGfip/VG
CVGfip = CGfip/PGfip
CLfip = ALfip/VL
CVLfip = CLfip/PLfip
mfs=cl_fip*CLfip
CFfip = AFfip/VF
CVFfip = CFfip/PFfip
CBRfip = ABRfip/VBR
CVBRfip = CBRfip/PBRfip
CRfip = ARfip/VR
CVRfip = CRfip/PRfip
CSfip = ASfip/VS
CVSfip = CSfip/PSfip
CKfip = AKfip/VK
CVKfip = CKfip/PKfip
Urine1= cl_renal* CKfip
CRPfip = ARPfip/VRP
CVRPfip = CRPfip/PRPfip
Egg1 = QEgg * CRPfip
CV1 = (QF*CVFfip + (QG+QL)*CVLfip + QBR*CVBRfip + QR*CVRfip + QS*CVSfip + QK*CVKfip +
QRP*CVRPfip)/QC
CA1 = ABfip/VB
CEggfip = AEgg1/VEgg

;fipronil sulfone
CGsul = AGsul/VG
CVGsul = CGsul/PGsul
CLsul = ALsul/VL
CVLsul = CLsul/PLsul
CFsul = AFsul/VF
CVFsul = CFsul/PFsul
CBRsul = ABRsul/VBR
CVBRsul = CBRsul/PBRsul
CRsul = ARsul/VR
CVRsul = CRsul/PRsul
CSsul = ASsul/VS
CVSsul = CSsul/PSsul
```

```
    CKsul = AKsul/VK
    CVKsul = CKsul/PKsul
    CRPsul = ARPsul/VRP
    CVRPsul = CRPsul/PRPsul
    Egg2 = QEgg * CRPsul
    C_Egg=AEgg2/0.0011875
    Egg_ex=C_Egg*0.002375
    CV2 = (QF*CVFsul + (QG+QL)*CVLsul + QBR*CVBRsul + QR*CVRsul + QS*CVSsul + QK*CVKsul +
QRP*CVRPsul)/QC
    CA2 = ABsul/VB

    ;fipronil (diff)
    Alu' = -Ka* Alu                 Init Alu = ODOSEmg*fa
    Absorb1' = Ka * Alu     Init Absorb1 = 0
    AGfip' = QG*(CA1-CVGfip) + Ka *Alu          Init AGfip = 0
    ALfip' = QL*(CA1-CVLfip) + QG*(CVGfip-CVLfip) - mfs                 Init ALfip = 0
    Ameta' = mfs                    Init Ameta = 0
    AFfip' = QF*(CA1-CVFfip)            Init AFfip = 0
    ABRfip' = QBR*(CA1-CVBRfip)         Init ABRfip = 0
    ARfip' = QR*(CA1-CVRfip)    Init ARfip = 0
    ASfip' = QS*(CA1-CVSfip)            Init ASfip = 0
    AKfip' = QK*(CA1-CVKfip)    -Urine1         Init AKfip = 0
    AUrine1' = Urine1               Init AUrine1 = 0
    ARPfip' = QRP*(CA1-CVRPfip)-Egg1    Init ARPfip = 0
    AEgg1' = Egg1                   Init AEgg1 =0
    ABfip' = QC*(CV1-CA1)           Init ABfip =0
    MassBal1' = Absorb1-
(Ameta+AGfip+ALfip+AFfip+ARfip+ASfip+AKfip+AUrine1+ARPfip+AEgg1+ABfip)
    Init MassBal1 = 0

    Totalfri = Absorb1
    Calculatedfri = (Ameta+AGfip+ALfip+AFfip+ARfip+ASfip+AKfip+AUrine1+ARPfip+AEgg1+ABfip)
    ERRORfri=(Totalfri-Calculatedfri)/(Totalfri+1E-30)*100
    MBfri=Totalfri-Calculatedfri + 1


    ;fipronil sulfone (diff)
    AGsul' = QG*(CA2-CVGsul)                    Init AGsul = 0
    ALsul' = QL*(CA2-CVLsul) + QG*(CVGsul-CVLsul) + mfs                 Init ALsul = 0
    Amfs' = mfs                     Init Amfs = 0
    AFsul' = QF*(CA2-CVFsul)            Init AFsul = 0
    ABRsul' = QBR*(CA1-CVBRsul)         Init ABRsul = 0
    ARsul' = QR*(CA2-CVRsul)    Init ARsul = 0
    ASsul' = QS*(CA2-CVSsul)            Init ASsul = 0
    AKsul' = QK*(CA2-CVKsul)            Init AKsul = 0
    ARPsul' = QRP*(CA2-CVRPsul)-Egg2    Init ARPsul = 0
    AEgg2' = Egg2-Egg_ex                Init AEgg2 =0
    AEgg3' = Egg_ex                 Init AEgg3 = 0
    ABsul' = QC*(CV2-CA2)           Init ABsul =0
    MassBal2' = Amfs-(AGsul+ALsul+AFsul+ARsul+ASsul+AKsul+ARPsul+AEgg2+AEgg3+ABsul)
    Init MassBal2 = 0
```

References

Authority (EFSA), E. F. S., Aagaard, A., Berny, P., Chaton, P.-F., Antia, A. L., McVey, E., Arena, M., Fait, G., Ippolito, A., Linguadoca, A., Sharp, R., Theobald, A., & Brock, T. (2023). Risk assessment for Birds and Mammals. *EFSA Journal*, *21*(2), e07790. https://doi.org/10.2903/j.efsa.2023.7790

Baier, V., Paini, A., Schaller, S., Scanes, C. G., Bone, A. J., Ebeling, M., Preuss, T. G., Witt, J., & Heckmann, D. (2022). A generic avian physiologically-based kinetic (PBK) model and its application in three bird species. *Environment International*, *169*, 107547.

Bhatt, P., Gangola, S., Ramola, S., Bilal, M., Bhatt, K., Huang, Y., Zhou, Z., & Chen, S. (2023). Insights into the toxicity and biodegradation of fipronil in contaminated environment. *Microbiological Research*, *266*, 127247. https://doi.org/10.1016/j.micres.2022.127247

Chiu, W. A., Barton, H. A., DeWoskin, R. S., Schlosser, P., Thompson, C. M., Sonawane, B., Lipscomb, J. C., & Krishnan, K. (2007). Evaluation of physiologically based pharmacokinetic models for use in risk assessment. *Journal of Applied Toxicology: An International Journal*, *27*(3), 218–237.

Corrias, F., Atzei, A., Taddeo, R., Arru, N., Casula, M., Salghi, R., Russo, M., & Angioni, A. (2021). Fipronil and fipronil sulfone distribution in chicken feathers and eggs after oral and dermal exposure. *Foods*, *10*(12), 3077.

Cortright, K. A., Wetzlich, S. E., & Craigmill, A. L. (2009). A PBPK model for midazolam in four avian species. *Journal of Veterinary Pharmacology and Therapeutics*, *32*(6), 552–565. https://doi.org/10.1111/j.1365-2885.2009.01073.x

Diepens, N. J., Belgers, D., Buijse, L., & Roessink, I. (2023). Pet dogs transfer veterinary medicines to the environment. *Science of the Total Environment*, *858*, 159550.

Dogruer, G., Kramer, N. I., Schaap, I. L., Hollert, H., Gaus, C., & van de Merwe, J. P. (2021). An integrative approach to define chemical exposure threshold limits for endangered sea turtles. *Journal of Hazardous Materials*, *420*, 126512. https://doi.org/10.1016/j.jhazmat.2021.126512

EFSA (European Food Safety Authority). (2009). Guidance on Risk Assessment for Birds and Mammals on request from EFSA. *EFSA Journal 2009, 7(12):1438*, 358 pp.

Fantke, P., Friedrich, R., & Jolliet, O. (2012). Health impact and damage cost assessment of pesticides in Europe. *Environment International*, *49*, 9–17. https://doi.org/10.1016/j.envint.2012.08.001

Fantke, P., & Jolliet, O. (2016). Life cycle human health impacts of 875 pesticides. *The International Journal of Life Cycle Assessment*, *21*(5), 722–733. https://doi.org/10.1007/s11367-015-0910-y

Fernie, K. J., Marteinson, S. C., Bird, D. M., Ritchie, I. J., & Letcher, R. J. (2011). Reproductive changes in American kestrels (Falco sparverius) in relation to exposure to technical hexabromocyclododecane flame retardant. *Environmental Toxicology and Chemistry*, *30*(11), 2570–2575. https://doi.org/10.1002/etc.652

Fipronil Environmental Effects. (n.d.).

Gerletti, P., Von Kleist, M., Mielke, H., Kuhl, T., Pieper, R., Lahrssen-Wiederholt, M., & Numata, J. (2020). Transfer kinetics of fipronil into chicken (*Gallus gallus domesticus*) eggs. *Computational Toxicology*, *15*, 100131. https://doi.org/10.1016/j.comtox.2020.100131

Halleux, V. (2023). Sustainable use of plant protection products. *EPRS | European Parliamentary Research Service*. https://www.europarl.europa.eu/RegData/etudes/ATAG/2023/754587/EPRS_ATA(2023)754587_EN.pdf

Horak, K. E., Fisher, P. M., & Hopkins, B. (2018). Pharmacokinetics of anticoagulant rodenticides in target and non-target organisms. *Anticoagulant Rodenticides and Wildlife*, 87–108.

Igado, O., & Aina, O. (2010). *Some aspects of the neurometrics and oculometrics of the japanese quail (Coturnix coturnix japonica) in Nigeria*. *27*, 133–135.

Jeschke, P. (2016). Progress of modern agricultural chemistry and future prospects. *Pest Management Science*, *72*(3), 433–455.

Jongeneelen, F. J., & Berge, W. F. T. (2011). A generic, cross-chemical predictive PBTK model with multiple entry routes running as application in MS Excel; design of the model and comparison of predictions with experimental results. *Annals of Occupational Hygiene*, *55*(8), 841–864. https://doi.org/10.1093/annhyg/mer075

Kawahara, T., & Saito, K. (1976). Genetic Parameters of Organ and Body Weights in the Japanese Quail*. *Poultry Science*, *55*(4), 1247–1252. https://doi.org/10.3382/ps.0551247

Khidkhan, K., Poapolathep, S., Kulprasertsri, S., Sukkheewan, R., Khunlert, P., Giorgi, M., & Poapolathep, A. (2022). Comparative in vitro biotransformation of fipronil in domestic poultry using liver microsome. *Journal of Veterinary Science*, *23*(6).

Kim, S., Chen, J., Cheng, T., Gindulyte, A., He, J., He, S., Li, Q., Shoemaker, B. A., Thiessen, P. A., Yu, B., Zaslavsky, L., Zhang, J., & Bolton, E. E. (2021). PubChem in 2021: New data content and improved web interfaces. *Nucleic Acids Research*, *49*(D1), D1388–D1395. https://doi.org/10.1093/nar/gkaa971

Kitulagodage, M. (2011). Impact of fipronil, a new generation pesticide, on avian development and health. *University of Wollongong Thesis Collection 1954-2016*. https://ro.uow.edu.au/theses/3523

Kitulagodage, M., Isanhart, J., Buttemer, W. A., Hooper, M. J., & Astheimer, L. B. (2011). Fipronil toxicity in northern bobwhite quail Colinus virginianus: Reduced feeding behaviour and sulfone metabolite formation. *Chemosphere*, *83*(4), 524–530.

Krishnan, K., & Peyret, T. (2009). Physiologically based toxicokinetic (PBTK) modeling in ecotoxicology. *Ecotoxicology Modeling*, 145–175.

Lautz, L. S., Nebbia, C., Hoeks, S., Oldenkamp, R., Hendriks, A. J., Ragas, A. M. J., & Dorne, J. L. C. M. (2020). An open source physiologically based kinetic model for the chicken (*Gallus gallus domesticus*): Calibration and validation for the prediction residues in tissues and eggs. *Environment International*, *136*, 105488. https://doi.org/10.1016/j.envint.2020.105488

Lautz, L. S., Stoopen, G., Ginting, A. J., Hoogenboom, R. L. A. P., & Punt, A. (2022). Fipronil and fipronil sulfone in chicken: From *in vitro* experiments to *in vivo* PBK model predictions. *Food and Chemical Toxicology*, *165*, 113086. https://doi.org/10.1016/j.fct.2022.113086

Li, Z. (2020). PBCLM: A top-down causal modeling framework for soil standards and global sustainable agriculture. *Environmental Pollution*, *263*, 114404. https://doi.org/10.1016/j.envpol.2020.114404

Lilienblum, W., Dekant, W., Foth, H., Gebel, T., Hengstler, J. G., Kahl, R., Kramer, P.-J., Schweinfurth, H., & Wollin, K.-M. (2008). Alternative methods to safety studies in experimental animals: Role in the risk assessment of chemicals under the new European Chemicals Legislation (REACH). *Archives of Toxicology*, *82*(4), 211–236. https://doi.org/10.1007/s00204-008-0279-9

Lu, J., Goldsmith, M.-R., Grulke, C. M., Chang, D. T., Brooks, R. D., Leonard, J. A., Phillips, M. B., Hypes, E. D., Fair, M. J., Tornero-Velez, R., Johnson, J., Dary, C. C., & Tan, Y.-M. (2016). Developing a Physiologically-Based Pharmacokinetic Model Knowledgebase in Support of Provisional Model Construction. *PLOS Computational Biology*, *12*(2), e1004495. https://doi.org/10.1371/journal.pcbi.1004495

MacLachlan, D. j. (2008). Transfer of fat-soluble pesticides from contaminated feed to poultry tissues and eggs. *British Poultry Science*, *49*(3), 290–298. https://doi.org/10.1080/00071660802123344

MacLachlan, D. J. (2008). Transfer of fat-soluble pesticides from contaminated feed to poultry tissues and eggs. *British Poultry Science*, *49*(3), 290–298. https://doi.org/10.1080/00071660802123344

Mahmoud, T. H., & Coleman, T. H. (1967). A Comparison of the Proportion of Component Parts of Bobwhite

and Coturnix Eggs1. *Poultry Science*, *46*(5), 1168–1171. https://doi.org/10.3382/ps.0461168

Mavroudis, P. D., Hermes, H. E., Teutonico, D., Preuss, T. G., & Schneckener, S. (2018). Development and validation of a physiology-based model for the prediction of pharmacokinetics/toxicokinetics in rabbits. *PLOS ONE*, *13*(3), e0194294. https://doi.org/10.1371/journal.pone.0194294

Ministerie van Landbouw, N. en V. (2017, August 16). *Rodenticides—Board for the Authorisation of Plant Protection Products and Biocides* [Onderwerp]. Ministerie van Landbouw, Natuur en Voedselkwaliteit. https://english.ctgb.nl/topics/rodenticides

Paini, A., Leonard, J. A., Joossens, E., Bessems, J. G. M., Desalegn, A., Dorne, J.-L., Gosling, J. P., Heringa, M. B., Klaric, M., & Kliment, T. (2019). Next generation physiologically based kinetic (NG-PBK) models in support of regulatory decision making. *Computational Toxicology*, *9*, 61–72.

Perkins, R., Barron, L., Glauser, G., Whitehead, M., Woodward, G., & Goulson, D. (2024). Down-the-drain pathways for fipronil and imidacloprid applied as spot-on parasiticides to dogs: Estimating aquatic pollution. *Science of The Total Environment*, *917*, 170175. https://doi.org/10.1016/j.scitotenv.2024.170175

Pletz, J., Blakeman, S., Paini, A., Parissis, N., Worth, A., Andersson, A.-M., Frederiksen, H., Sakhi, A. K., Thomsen, C., & Bopp, S. K. (2020). Physiologically based kinetic (PBK) modelling and human biomonitoring data for mixture risk assessment. *Environment International*, *143*, 105978.

Punt, A., Louisse, J., Pinckaers, N., Fabian, E., & van Ravenzwaay, B. (2022). Predictive performance of next generation physiologically based kinetic (PBK) model predictions in rats based on in vitro and in silico input data. *Toxicological Sciences*, *186*(1), 18–28.

Regulation 1107/2009. (n.d.). *Regulation (EC) No 1107/2009 of the European Parliament and of the Council of 21 October 2009 Concerning the Placing of Plant Protection Products on the Market and Repealing*. https://eur-lex.europa.eu/LexUriServ/LexUriServ.do?uri=OJ:L:2009:309:0001:0050:en:PDF

Rietjens, I. M., Louisse, J., & Punt, A. (2011). Tutorial on physiologically based kinetic modeling in molecular nutrition and food research. *Molecular Nutrition & Food Research*, *55*(6), 941–956.

Rowland, M., Peck, C., & Tucker, G. (2011). Physiologically-Based Pharmacokinetics in Drug Development and Regulatory Science. *Annual Review of Pharmacology and Toxicology*, *51*(Volume 51, 2011), 45–73. https://doi.org/10.1146/annurev-pharmtox-010510-100540

Shebley, M., Sandhu, P., Emami Riedmaier, A., Jamei, M., Narayanan, R., Patel, A., Peters, S. A., Reddy, V. P., Zheng, M., de Zwart, L., Beneton, M., Bouzom, F., Chen, J., Chen, Y., Cleary, Y., Collins, C.,

Dickinson, G. L., Djebli, N., Einolf, H. J., … Rowland, M. (2018). Physiologically Based Pharmacokinetic Model Qualification and Reporting Procedures for Regulatory Submissions: A Consortium Perspective. *Clinical Pharmacology & Therapeutics*, *104*(1), 88–110. https://doi.org/10.1002/cpt.1013

Spaiser, V., Ranganathan, S., Swain, R. B., & Sumpter, D. J. T. (2017). The sustainable development oxymoron: Quantifying and modelling the incompatibility of sustainable development goals. *International Journal of Sustainable Development & World Ecology*, *24*(6), 457–470. https://doi.org/10.1080/13504509.2016.1235624

Strikwold, M., Spenkelink, B., Woutersen, R. A., Rietjens, I. M., & Punt, A. (2013). Combining in vitro embryotoxicity data with physiologically based kinetic (PBK) modelling to define in vivo dose–response curves for developmental toxicity of phenol in rat and human. *Archives of Toxicology*, *87*, 1709–1723.

Szabo, J. K., Davy, P. J., Hooper, M. J., & Astheimer, L. B. (2009). Predicting avian distributions to evaluate spatiotemporal overlap with locust control operations in eastern Australia. *Ecological Applications*, *19*(8), 2026–2037. https://doi.org/10.1890/08-0264.1

Tan, Y.-M., Worley, R. R., Leonard, J. A., & Fisher, J. W. (2018). Challenges Associated With Applying Physiologically Based Pharmacokinetic Modeling for Public Health Decision-Making. *Toxicological Sciences*, *162*(2), 341–348. https://doi.org/10.1093/toxsci/kfy010

Thompson, C. V., Firman, J. W., Goldsmith, M. R., Grulke, C. M., Tan, Y.-M., Paini, A., Penson, P. E., Sayre, R. R., Webb, S., & Madden, J. C. (2021). A Systematic Review of Published Physiologically-based Kinetic Models and an Assessment of their Chemical Space Coverage. *Alternatives to Laboratory Animals*, *49*(5), 197–208. https://doi.org/10.1177/02611929211060264

UN General Assembly. (2015, October 21). *Transforming our world: The 2030 Agenda for Sustainable Development*. https://www.refworld.org/legal/resolution/unga/2015/en/111816

US EPA. (1996). New pesticide fact sheet. *Office of Pesticide Programs Washington, DC*. https://nepis.epa.gov/Exe/ZyNET.exe/P1001KCY.txt?ZyActionD=ZyDocument&Client=EPA&Index=1995%20Thru%201999&Docs=&Query=&Time=&EndTime=&SearchMethod=1&TocRestrict=n&Toc=&TocEntry=&QField=&QFieldYear=&QFieldMonth=&QFieldDay=&UseQField=&IntQFieldOp=0&ExtQFieldOp=0&XmlQuery=&File=D%3A%5CZYFILES%5CINDEX%20DATA%5C95THRU99%5CTXT%5C00000021%5CP1001KCY.txt&User=ANONYMOUS&Password=anonymous&SortMet

hod=h%7C-

&MaximumDocuments=1&FuzzyDegree=0&ImageQuality=r75g8/r75g8/x150y150g16/i425&Display=hpfr&DefSeekPage=x&SearchBack=ZyActionL&Back=ZyActionS&BackDesc=Results%20page&MaximumPages=1&ZyEntry=2#

US EPA, O. (2023, January 9). *Toxicokinetics Overview* [Overviews and Factsheets]. https://www.epa.gov/chemical-research/toxicokinetics-overview